

## HEAT CONDUCTION AND HEAT TRANSFER IN TECHNOLOGICAL PROCESSES

### FINITE-ELEMENT MODEL OF TEMPERATURE CONDITIONS IN SELF-PROPAGATING HIGH-TEMPERATURE SYNTHESIS OF CYLINDRICAL BLANKS

V. L. Kvanin, N. T. Balikhina, P. I. Krasnoshchekov,  
V. P. Radchenko, and A. F. Fedotov

UDC 621.1.016.4

*Two-dimensional, nonstationary heat-conduction problems in a system of four finite bodies with an internal mobile heat source of the first kind (burning front) have been solved by the finite-element method. The influence of basic technological factors on the temperature-field parameters in the process of synthesis of TiB–40% Ti alloys has been investigated. It has been shown that for a real technological cycle the temperature field in a blank and a sand shell can be considered to be stationary and homogeneous.*

A highly effective method for obtaining materials on the basis of refractory compounds is self-propagating high-temperature synthesis (SHS), which is a kind of combustion. To obtain high-density materials and products, combustion products of SHS heated by the combustion wave are subjected to force compaction. Of the flow diagrams of force compaction of uncooled products of synthesis, pressing in a closed matrix, or SHS-pressing is of the widest application. At present, the technology of obtaining products of simple shape in the form of plates or rings by the SHS method has been developed fairly well [1]. Therefore, the development of SHS-pressing flow diagrams for obtaining products of complex shape is topical. One such flow diagram is the process of radial SHS-pressing of cylindrical products.

The basic flow diagram of the process of radial SHS-pressing is shown in Fig. 1. The charge blank has the form of a circular cylinder and represents a pressed briquette from an isothermal mixture of powders. The axis of the cylinder is horizontal and it is positioned, to a depth of half of its diameter, in a cylindrical channel on the bottom of a rigid matrix. The pressing pressure is transferred to the cylinder through a sand shell. The SHS process is initiated from the face of the charge blank, and the burning front moves along the blank axis. Upon completion of synthesis there occurs pressing of hot SHS products together with the sand shell throughout the charge volume. The capacity of synthesis products for plastic deformation and compaction is primarily due to the deformation temperature. In this connection, investigations of the temperature conditions under radial SHS-pressing are of scientific and practical interest.

Unlike hot pressing of inert powders under which, due to external heating, isothermal conditions are created, under SHS pressing there occurs continuous cooling of a deformable material. Therefore, heat insulation of synthesis products from the cold deforming tool has to be provided. Moreover, the SHS process is followed by a release of gases that were adsorbed or dissolved in the initial components of the charge and it is necessary to ensure removal of the gases from the mould. In the case of radial SHS pressing the problem is solved as follows. For heat insulation and removal of impurity gases the upper part of the blank is placed in a gas-permeable sand shell (Fig. 1). Heat insulation of the lower part of the blank, situated in the cylindrical channel on the bottom of the matrix, is provided by a tape heat insulator — glass cloth. Thus, in the case of radial SHS pressing a nonhomogeneous heat insulator is used and on the blank surface asymmetric boundary conditions of the fourth kind take place.

The known works on the temperature regime in the force-compaction SHS considered the problem of nonstationary heat transfer with burning-front propagation along the cylinder axis without consideration for the heat insulator

---

Samara State Technical University, 244 Molodogvardeiskaya Str., Samara, 443100, Russia. Translated from *Inzhenerno-Fizicheskii Zhurnal*, Vol. 79, No. 5, pp. 64–73, September–October, 2006. Original article submitted February 25, 2005.

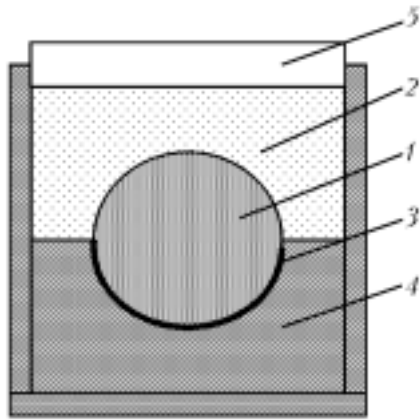


Fig. 1. Schematic diagram of radial SHS pressing: 1) blank; 2) shell; 3) tape heat insulator; 4) matrix; 5) die.

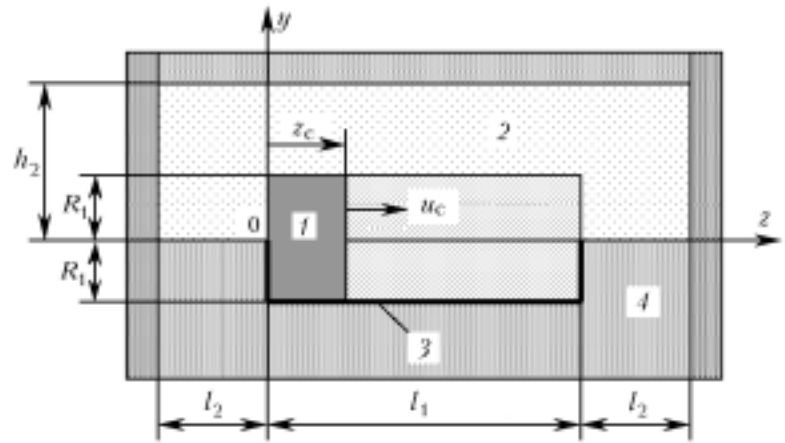


Fig. 2. Design diagram of the object of modeling in the longitudinal section of the blank.

[2] or perpendicularly to the axis of a flat blank with a homogeneous heat insulator [3]. The aim of the present work is to develop a mathematical model and elucidate the mechanisms of formation of temperature conditions in the SHS of a cylindrical blank with a nonhomogeneous heat insulator.

When the burning front propagates from the face of the charge blank, the heat transfer between the synthesis products and the environment occurs in the direction of three space coordinates. The dimension of the temperature field formed at the stage of synthesis determines also the dimension of the problem of plastic deformation at the pressing stage. The solution of three-dimensional, nonstationary heat-conduction and plasticity problems for a system of several bodies is mathematically awkward and laborious. Therefore, in theoretical and applied studies researchers restrict themselves, as a rule, to the analysis of two-dimensional or axially symmetric mathematical models, which permit fairly complete elucidation and investigation of the basic mechanisms of the physical process. To this end, it is enough to consider the shaping of the article being pressed in its plane longitudinal and transverse sections. Accordingly, in the present work we investigated the process of heat transfer in a two-dimensional system for the two characteristic sections of a cylindrical blank — the longitudinal and transverse sections.

Let us first investigate the process of heat transfer in the longitudinal section. By analogy with [3], for this section the heat transfer of a two-dimensional layer of unit thickness with perfect heat insulation of the lateral faces was considered. The physical formulation of the problem is as follows.

A 2-D layer of unit thickness is placed in a homogeneous heat insulator and a steel tool also of unit thickness. The dimensions of the layer, the heat insulator, and the tool are known. At the initial instant of time, at the layer end the reaction of combustion with known combustion temperature  $T_c$  and rate of combustion  $u_c$  is initiated. The heat exchange of the synthesis products with the heat insulator and of the heat insulator with the tool occurs at boundary conditions of the fourth kind with a perfect thermal contact. At the tool–environment interface boundary, conditions of the third kind take place. There is no heat transfer on the lateral faces of the layer, the heat insulator, and the tool. The burning front is assumed to be plane and adiabatic. The temperature dependence of the thermophysical properties of the materials is neglected. It is required to find the temperature field of the system at an arbitrary instant of time  $t$ .

Figure 2 shows the design diagram of a two-dimensional, four-element system consisting of synthesis products 1, a sand shell 2, a tape heat insulator 3, and a steel tool 4. Combustion of the layer begins from the left end surface ( $z_0 = 0$ ); the plane burning front moves at a constant rate  $u_c$  in the direction of the blank axis  $z$ .

The mathematical model of the heat transfer at the combustion stage includes:

1) the system of four differential nonstationary heat-conduction equations in Cartesian coordinates  $z$  and  $y$ :

$$c_i \rho_i \frac{\partial T_i(z, y, t)}{\partial t} = \lambda_i \left( \frac{\partial^2 T_i(z, y, t)}{\partial z^2} \right) + \lambda_i \left( \frac{\partial^2 T_i(z, y, t)}{\partial y^2} \right); \quad (1)$$

2) at the blank–heat insulator and heat insulator–tool interfaces, the boundary conditions of the fourth kind

$$\begin{aligned}
\lambda_1 \frac{\partial T_1(z_{1-2}, y_{1-2}, t)}{\partial n} &= \lambda_2 \frac{\partial T_2(z_{1-2}, y_{1-2}, t)}{\partial n}, \quad T_1(z_{1-2}, y_{1-2}, t) = T_2(z_{1-2}, y_{1-2}, t); \\
\lambda_1 \frac{\partial T_1(z_{1-3}, y_{1-3}, t)}{\partial n} &= \lambda_3 \frac{\partial T_3(z_{1-3}, y_{1-3}, t)}{\partial n}, \quad T_1(z_{1-3}, y_{1-3}, t) = T_3(z_{1-3}, y_{1-3}, t); \\
\lambda_2 \frac{\partial T_2(z_{2-3}, y_{2-3}, t)}{\partial n} &= \lambda_3 \frac{\partial T_3(z_{2-3}, y_{2-3}, t)}{\partial n}, \quad T_2(z_{2-3}, y_{2-3}, t) = T_3(z_{2-3}, y_{2-3}, t); \\
\lambda_2 \frac{\partial T_2(z_{2-4}, y_{2-4}, t)}{\partial n} &= \lambda_4 \frac{\partial T_4(z_{2-4}, y_{2-4}, t)}{\partial n}, \quad T_2(z_{2-4}, y_{2-4}, t) = T_4(z_{2-4}, y_{2-4}, t); \\
\lambda_3 \frac{\partial T_3(z_{3-4}, y_{3-4}, t)}{\partial n} &= \lambda_4 \frac{\partial T_4(z_{3-4}, y_{3-4}, t)}{\partial n}, \quad T_3(z_{3-4}, y_{3-4}, t) = T_4(z_{3-4}, y_{3-4}, t);
\end{aligned} \tag{2}$$

at the tool–environment interface, the boundary conditions of the third kind

$$\lambda_4 \frac{\partial T_4(z, y, t)}{\partial n} + \alpha (T_4 - T_{\text{en}}) = 0; \tag{3}$$

3) the initial conditions

$$T_1(0, y, 0) = T_c, \quad T_2(z, y, 0) = T_{\text{en}}, \quad T_3(z, y, 0) = T_{\text{en}}, \quad T_4(z, y, 0) = T_{\text{en}}; \tag{4}$$

4) the equation of motion of the burning front

$$z_c = u_c t; \tag{5}$$

5) the temperature of the mobile boundary of the first kind (burning front)

$$T_1(z_c, y, t) = T_c; \tag{6}$$

6) the adiabaticity conditions before the burning front ( $z = z_c + 0$ )

$$\frac{\partial T_1(z_c + 0, y, t)}{\partial z} = 0. \tag{7}$$

In calculating the temperature field upon complete combustion of the layer, Eqs. (5)–(7) are eliminated from the system of equations (1)–(7) and the boundary conditions of the fourth kind on the right end surface of the layer

$$\begin{aligned}
\lambda_1 \frac{\partial T_1(l_1, y, t)}{\partial z} &= \lambda_2 \frac{\partial T_2(l_1, y, t)}{\partial z}, \quad T_1(l_1, y, t) = T_2(l_1, y, t); \\
\lambda_1 \frac{\partial T_1(l_1, y, t)}{\partial z} &= \lambda_3 \frac{\partial T_3(l_1, y, t)}{\partial z}, \quad T_1(l_1, y, t) = T_3(l_1, y, t).
\end{aligned}$$

The formulated boundary-value, nonstationary, heat-conduction problem was solved by the finite-element method (FEM) with minimization of the variational functional [4]

$$J = \sum_{i=1}^4 \frac{1}{2} \int_{V_i} \left[ \lambda_i \left( \frac{\partial T_i}{\partial z} \right)^2 + \lambda_i \left( \frac{\partial T_i}{\partial y} \right)^2 + 2c_i \rho_i \frac{\partial T_i}{\partial t} T_i \right] dV_i + \int_{S_4} \frac{\alpha}{2} (T_4 - T_{\text{en}})^2 dS. \quad (8)$$

Triangular finite elements with a linear approximation of the temperature inside the element were used. The distinguishing feature of functional (8) is the fact that at the combustion stage the volume  $V_1$  of hot synthesis products with which heat exchange occurs is the time function

$$V_1 = 2R_1 u_c t.$$

The stationarity condition of functional (8) leads to the following discrete differential equation in matrix form:

$$[C] \frac{\partial \{T\}}{\partial t} + [\Lambda] \cdot \{T\} = \{F\}. \quad (9)$$

The matrix differential equation (9) was solved by the finite-difference method according to the implicit "backward" difference scheme

$$([C] + \Delta t [\Lambda]) \cdot \{T_k\} = [C] \cdot \{T_{k-1}\} + \Delta t \cdot \{F\}. \quad (10)$$

The matrix elements  $[C]$ ,  $[\Lambda]$ , and  $\{F\}$  were determined from the known dependences for plane triangular elements [4].

The dimensions of the grid elements of the discrete model were obtained in analyzing the results of the numerical solution for convergence to the exact solution of the boundary-value problem. The problem under consideration has no analytical solution. Therefore, to determine optimal steps by the time axis and space coordinates, we compared the numerical and analytical solutions of the one-dimensional problem on the cooling of an infinite layer from SHS products in an unbounded sand medium at boundary conditions of the fourth kind [5]. It has been established that a discrepancy of 1% is obtained at a thickness of the heat-insulator contact layer of 0.25 mm. The thickness of the following two layers is 0.75 and 2 mm. In the blank, the thickness of the first three layers, beginning with the contact layer, is 0.5, 1.5, and 2 mm, respectively. The value of the time step  $\Delta t$  should not be larger than  $\Delta t = 0.1\text{--}0.2$  sec.

The propagation of the burning front in the longitudinal direction was simulated by increasing stepwise the number of finite elements of the blank participating in the heat exchange. The longitudinal section consists of rectangular bodies, and we used a base rectangular grid of finite elements in which rectangles are divided by diagonals into two triangles. Therefore, the whole region represents a set of vertical columns and horizontal layers. In the approximation of the plane burning front, in one step the volume of the synthesized material increases by the volume of elements of one column of the blank. In the first step, only elements of the first column of the blank of width  $\Delta z_1$  participate in the heat exchange. In the second step, the burning front moves over a distance equal to the width of elements of the second column of the blank  $\Delta z_2$ ; in the third step it moves over a distance equal to the width of elements of the third column of the blank  $\Delta z_3$ , and so on. In the  $k$ th step, the combustion time  $t_{ck}$  of a new column of the blank of width  $\Delta z_k$  is

$$\Delta t_{ck} = \frac{\Delta z_k}{u_c}.$$

During this time, cooling of the synthesized volume of the blank also occurs. In each  $k$ th step of combustion the contact temperature  $T_{\text{con}0}$  of the newly formed blank-shell contact surface is unknown. Therefore, first the temperature  $T_{\text{con}0}$  of the new contact units was calculated by Eqs. (10) at time  $\Delta t = 10^{-6}$  sec, and then these equations were solved with a step  $\Delta t_{ck}$  and the temperature field at the current instant of time was determined. The system of linear equations (10) was solved by the Seidel method with an accuracy of  $0.01^\circ\text{C}$ .

The mechanisms of temperature-field formation under SHS of a cylindrical blank were studied for the Ti-12 mass% B SHS system with the formation of a solid TiB-40 mass% Ti alloy. The combustion temperature  $T_c$  is higher than the eutectic temperature of the TiB-Ti system, equal to  $1667^\circ\text{C}$  [6], but lower than the melting temperature of

TABLE 1. Thermophysical Properties of Materials and Thermokinetic Parameters of Combustion

Material	$\lambda$ , W/(m·K)	$c$ , J/(kg·K)	$\rho$ , kg/m <sup>3</sup>
TiB–40% Ti	13.5	939	2490
Sand [10]	0.326	795	1500
Glass cloth [10, 11]	0.048	837	150
Steel [10]	32	561	7800

Note. For TiB–40 mass% Ti,  $T_c = 1800^\circ\text{C}$ ,  $u_c = 5$  mm/sec.

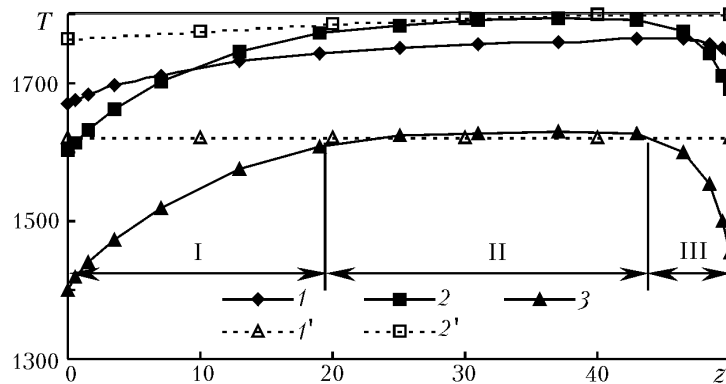


Fig. 3. Change in the temperature of the upper contact surface  $T_{\text{con.up}}$  (1, 1'), the center  $T_{\text{cen}}$  (2, 2'), and the lower contact surface  $T_{\text{con.l}}$  (3) in the longitudinal section of the blank: 1–3) solution by the FEM of the two-dimensional problem; 1' and 2') analytical solution of the one-dimensional problem.  $T$ ,  $^\circ\text{C}$ ;  $z$ , mm.

titanium monoboride, equal to  $2189^\circ\text{C}$  [7], and the synthesis products consist of solid particles of titanium monoboride and boride–titanium melt. The thermophysical properties of the porous solid–liquid material were calculated by the relations of [8] and the quantity of the solid and liquid phases and the composition of the melt, as well as the porosity of the material, equal to 50%, were taken into account in accordance with the state diagram. In the reference literature, there is a lack of data on the heat-conductivity coefficient and the specific heat capacity for glass cloth, but there is information on the thermophysical properties of various glass-fiber materials [9, 10] depending on the material density. The density of the glass cloth used was  $\rho_3 \approx 150$  kg/m<sup>3</sup>, and for this value we determined, using the reference data of [9, 10], the heat-conductivity coefficient and the specific heat capacity of the glass cloth (see Table 1). The data on the combustion temperature  $T_c$  and the rate of combustion  $u_c$  were obtained experimentally. The heat-transfer coefficient was taken to be equal to  $\alpha = 44$  W/(m<sup>2</sup>·K). The synthesis of a blank of radius  $R_1 = 18.5$  mm and length  $l_1 = 50$  mm was considered. The height of the sand shell  $h_2 = 38.5$  mm, the width  $l_2 = 12$  mm; the thickness of one layer of the glass cloth  $h_3 = 0.5$  mm; the tool thickness  $h_4 = 15$  mm.

The temperature field is formed during the combustion time and the pressing-delay time  $t_d$ , which is the pause between the moment the combustion terminates and the moment the pressing begins. For a blank of the given dimensions the combustion is constant and the varied time parameter is the pressing-delay time. To provide the maximum deformation temperature and the maximum degree of compaction of the synthesized material, the technological cycle should have the minimum pressing delay time [11]. The hydraulic presses and control systems used for SHS pressing of products ensure a technological cycle with a minimum pressing-delay time  $t_d = 1$ –2 sec. Subsequently, the minimum value of the delay time was assumed to be equal to  $t_d = 1$  sec.

Figure 3 shows the temperature distribution along the length of the longitudinal section of the blank upon synthesis of the TiB–40 mass% Ti alloy with a pressing delay time  $t_d = 1$  sec and a two-layer tape heat insulator of thickness  $h_3 = 1$  mm. The character of the temperature change on the lower  $T_{\text{con.l}}$  and upper  $T_{\text{con.up}}$  contact surfaces and at the center  $T_{\text{cen}}$  shows that in the blank an inhomogeneous temperature-field is formed. The temperature-field inhomogeneity is due to two factors. First, the flat layer of finite length has four boundaries of contact heat transfer,

which are heat sinks: two face and two bearing surfaces. Near these boundaries the "coldest" zones with a high temperature gradient are formed. Second, under layer-by-layer heating of the blank by the moving burning front the cooling time  $t_{\text{cool}}$  of individual zones depends on their position ( $z$ -coordinate) relative to the ignition plane:

$$t_{\text{cool}} = \frac{l_1 - z}{u_c} + t_d, \quad 0 \leq z \leq l_1. \quad (11)$$

Farther and farther away from the ignition plane and with increasing  $z$ -coordinate, the cooling time decreases and the blank temperature increases.

The temperature distribution in the longitudinal section of the blank under SHS in an inhomogeneous heat insulator is analogous to that under synthesis in a homogeneous heat insulator [3]. In both cases, upon termination of synthesis in the longitudinal section of the blank, three characteristic temperature zones connected with the corresponding boundary of contact heat transfer are formed (Fig. 3).

In the vicinity of the ignition plane ( $z = 0$ ), zone I is situated. The cooling time for this zone is the largest and it is the "coldest." The temperature on the contact surfaces and at the layer center increases with increasing distance from the ignition plane, and decreasing cooling time. At a certain distance from the ignition plane, the action of this boundary as a heat sink is leveled and zone II is formed. In this zone, the contact temperatures  $T_{\text{con.up}}$  and  $T_{\text{con.l}}$  weakly depend on the  $z$ -coordinate and cooling time — throughout the zone  $T_{\text{con.up}} \approx \text{const}$  and  $T_{\text{con.l}} \approx \text{const}$ . It was shown in [3] that in zone II internal cooling occurs [5] when the temperature of the contact surface behind the burning front remains constant and temperature homogenization throughout the blank volume occurs. In zone II, the contact temperature at the boundary where the blank contacts the sand shell  $T_{\text{con.up}}$  is approximately equal to the temperature  $T_{\text{con0}}$  that settles instantaneously at the boundary of contact of an infinite layer with temperature  $T_c$  placed in an infinite homogeneous medium with temperature  $T_{\text{en}}$  [5]:

$$T_{\text{con0}} = T_{\text{en}} + (T_c - T_{\text{en}}) \frac{K_1}{K_1 + K_h}.$$

For the sand shell the initial contact temperature is  $T_{\text{con0}} = 1622^\circ\text{C}$ ; the contact temperature  $T_{\text{con.up}}$  at the blank–sand shell interface in zone II is within the range  $T_{\text{con.up}} = 1620\text{--}1630^\circ\text{C}$ . The contact temperature at the boundary of the blank with the tape heat insulator, equal to  $T_{\text{con.l}} = 1750\text{--}1764^\circ\text{C}$ , differs markedly from the temperature  $T_{\text{con0}}$  for the infinite medium from glass cloth,  $T_{\text{con0}} = 1776^\circ\text{C}$ . The tape heat insulator and the steel tool represent, in the aggregate, a two-layer medium. The effective thermophysical properties of the two-layer medium differ from the individual properties of the bodies forming it, and this determines the difference between the temperatures  $T_{\text{con.l}}$  for the two-layer medium and  $T_{\text{con0}}$  for the homogeneous one.

In the region of the right end plane ( $z = l_1$ ) zone III is formed. This zone is characterized by a sharp decrease in the temperatures  $T_{\text{con.up}}$ ,  $T_{\text{con.l}}$ , and  $T_{\text{cen}}$  as the right end boundary of contact heat transfer, at which combustion has terminated, is approached. The cooling time of the right end and its adjoining volumes is much shorter than the cooling time of the left end and its adjoining volumes of the blank. As a result, the dimensions of zone III are smaller than those of zone I, and zone III has a higher temperature.

The results of the numerical solution were compared to the data of the analytical solution of the one-dimensional problem on the cooling of an infinite layer placed in an infinite homogeneous medium [5]. As the latter, sand is considered. The cooling time of the infinite layer was assumed to be equal to the cooling time of the section with a variable  $z$ -coordinate under combustion of an infinite-length layer and was calculated by relation (11). The results of the analytical solution and of the FEM solution (Fig. 3) for zone II are practically identical (the difference does not exceed 1%). From this it follows that the temperature field in zone II with internal cooling conditions arises from the one-dimensional contact heat transfer on the plane of support of the blank. Moreover, convergence of the numerical solution to the analytical solution for the assumed dimensions of the FE grid is confirmed.

Of practical interest is the choice of the number of layers of the tape heat insulator. Figure 4 shows the influence of the number of glass-cloth layers of thickness 0.5 mm on the temperature distribution along the lower contact surface of the blank  $T_{\text{con.l}}(z)$ . With increasing number of glass-cloth layers the heat removal decreases and the temperature of the contact surface of the blank increases. The results of the calculations have shown that an increase

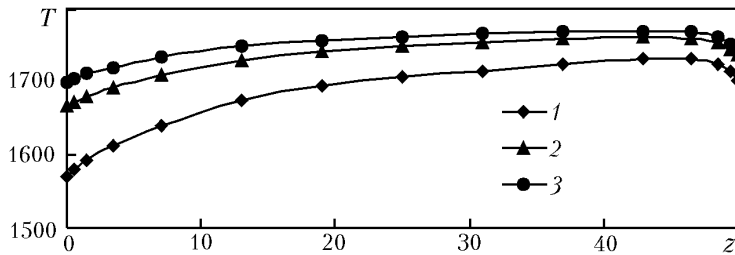


Fig. 4. Influence of the number of glass-cloth layers on the contact temperature  $T_{\text{con},l}$  distribution along the length of the longitudinal section of the blank at  $t_d = 1$  sec.  $T_{\text{con},l}$ , °C;  $z$ , mm.

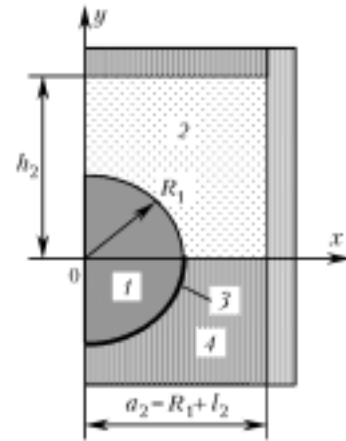


Fig. 5. Design diagram of the object of modeling in the cross section: 1) synthesis product; 2) sand shell; 3) tape heat insulator; 4) steel tool.

in the number of layers from two to three does not lead to a considerable increase in the temperature  $T_{\text{con},l}$ . Therefore, in the real process we can restrict ourselves to two glass-cloth layers with a total thickness of the tape heat insulator  $h_3 = 1$  mm.

Consider the heat-transfer process in the cross section of the blank. In zones I and III of the longitudinal section of the blank, three-dimensional heat transfer occurs. Therefore, we restrict ourselves to the investigation of the temperature conditions in zone II, where the heat transfer along the blank axis can be neglected and the heat transfer of a cylindrical blank of unit thickness with perfect heat insulation of the flat bases can be considered. In the process of motion of the plane burning front, the cross sections are instantaneously and uniformly heated to the combustion temperature and then their cooling occurs. The physical formulation of the problem is as follows.

A flat circular blank of radius  $R_1$  is placed in an inhomogeneous heat insulator and a steel tool with known parameters. At the initial instant of time, the blank temperature is equal to the combustion temperature  $T_c$ ; the temperature of the heat insulator and the tool is equal to the environment temperature  $T_{\text{en}}$ . The heat transfer between the synthesis products and the heat insulator and between the heat insulator and the tool occurs under boundary conditions of the fourth kind with perfect thermal contact. At the tool–environment interface, convective heat transfer occurs. There is no heat transfer on the flat bases of the blank, the heat insulator, and the tool. It is required to find the temperature field of the system at an arbitrary instant of time  $t$ . The design diagram is shown in Fig. 5. Because of the axial symmetry, we consider half of the cross section in Cartesian coordinate  $x$  and  $y$ .

The mathematical formulation of the problem of plane heat transfer includes:

- 1) the system of four differential nonstationary heat-conduction equations (1) in Cartesian coordinate  $x$  and  $y$ ;
- 2) the boundary conditions: a) of the fourth kind (2) at the blank–heat insulator and heat-insulator–tool interfaces; b) of the third kind (3) at the tool–environment interface;
- 3) the initial conditions

$$T_1(x, y, 0) = T_c, \quad T_2(x, y, 0) = T_{\text{en}}, \quad T_3(x, y, 0) = T_{\text{en}}, \quad T_4(x, y, 0) = T_{\text{en}}.$$

The boundary-value, nonstationary heat-transfer problem in the cross section was also solved by the FEM. As in the case of the longitudinal section, we used triangular elements and analogous dimensions of the contact layers of the blank and heat insulators. We considered the cross section situated at the center of zone II with internal cooling conditions with the coordinate  $z = 32$  mm and the cooling time  $t_{\text{cool}} = 4.6$  sec at  $t_d = 1$  sec.

Figure 6 shows the temperature distribution over the width ( $x$ -coordinate) and height ( $y$ -coordinate) of the blank cross section under consideration. The temperature of the calculation points decreases monotonically with in-

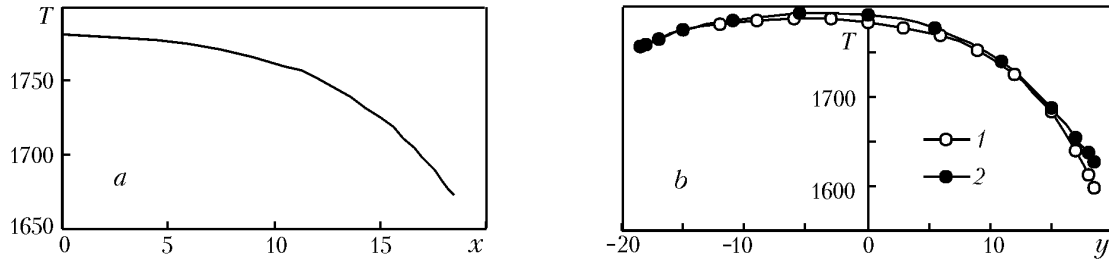


Fig. 6. Temperature distribution over the width (a) and height (b) of the cross section of the blank with  $z = 32$  mm and  $t_{\text{cool}} = 4.6$  sec: 1) solution of the problem for the cross section; 2) for the longitudinal section.  $T$ , °C;  $x$ ,  $y$ , mm.

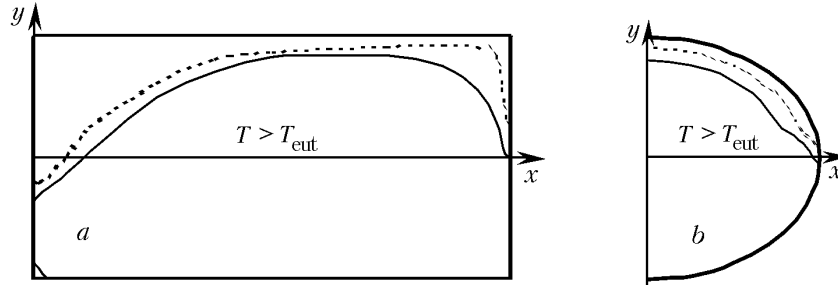


Fig. 7. Calculated isotherms  $T = T_{\text{eut}}$  in the longitudinal section (a) and the cross section (b) of the blank:  $t_d = 1$  and 5 sec (dotted and solid lines, respectively).

creasing distance from the center and with approach to the contact surface of the blank. Due to the smaller heat conduction of the glass cloth compared to the sand, the temperature of the volumes situated in the tape heat insulator ( $y < 0$ ) is higher than the temperature of the volumes situated in the sand shell ( $y > 0$ ). Figure 6b compares the temperature distributions over the blank height  $T(y)$  obtained from the solution of the heat-transfer problems that are independent of each other in the transverse and longitudinal sections. The good agreement between the  $T(y)$  dependences confirms the correctness of the physical models used (combustion of the flat layer and cooling of the cylindrical blank of unit thickness) for evaluating the temperature field in the longitudinal and transverse sections of the blank.

Under SHS pressing, there occurs continuous cooling of products obtained, and of practical interest is the estimation of the temperature–time parameters at which, under nonisothermal conditions, nonporous materials can be obtained. Let us estimate the time limits of the cooling process at the pressing stage. In working on hydraulic presses at a velocity of travel of the ram of 5–10 mm/sec, the deformation time of the synthesized blank is 1.5–3 sec. With allowance for the minimum necessary delay time  $t_d = 1$ –2 sec, the change in the temperature and in the temperature-dependent properties occurs in the time interval  $t_d = 1$ –5 sec.

It is customary to assume that the necessary condition for obtaining nonporous SHS materials is the presence of the liquid phase in the process of force compaction [12, 13]. Accordingly, the deformation temperature should be higher than the eutectic temperature of the synthesized alloy and the dimensions of zones with a temperature above  $T_{\text{eut}}$  permit predicting the size of the volume of a high-density material. Figure 7 shows the calculated isotherms  $T = T_{\text{eut}} = 1667^\circ\text{C}$  for the longitudinal section and transverse sections of the blank from the TiB–40 mass% Ti alloy. The region with  $T \geq T_{\text{eut}}$  and the solid-liquid state of the alloy is inside the blank. As would be expected, with increasing pressing-delay time  $t_d$  and, therefore, cooling time, the dimensions of the region with the solid-liquid state of the alloy decrease. However, the rate of cooling of the blank is low and as the pressing delay time increases from  $t_d = 1$  sec to  $t_d = 5$  sec, the dimensions of the region with  $T \geq T_{\text{eut}}$  decrease by no more than 10%. Thus, the high heat-insulation properties of the sand and glass cloth ensure the presence of the solid-liquid state of the alloy in fairly large volumes during the whole technologically required time. It should be noted that the temperature conditions determine only the level of temperature-dependent properties. Therefore, the final results for the pressed blank density can be obtained from the solution of the boundary-value problem of plastic deformation.



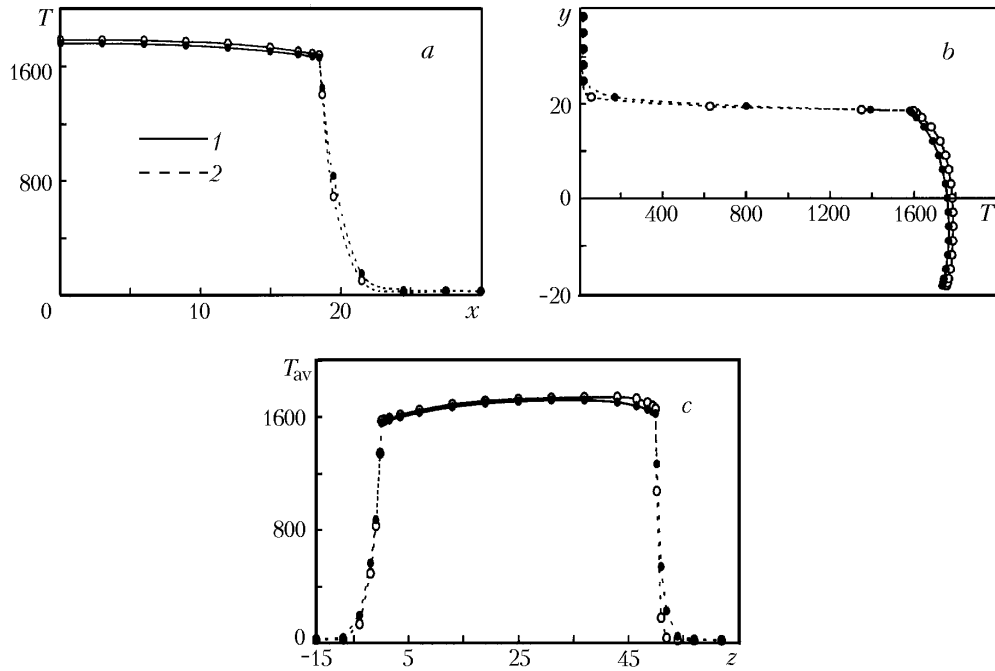


Fig. 8. Temperature distribution in the blank and the shell over the width (a) and height (b) of the cross section and average temperature distribution over the length of the longitudinal section (c): open circles denote the time delay  $t_d = 1$  sec, solid lines — the time delay  $t_d = 5$  sec; 1) blank; 2) shell.  $T$ ,  $T_{av}$ , °C;  $x$ ,  $y$ ,  $z$ , mm.

In describing the process of plastic deformation of cooling-down SHS products, an important question is how correctly the approximation of the isothermal and homogeneous field can be used. To answer this question, it is necessary to consider the character of the temperature distribution in the blank and in the shell and its time dynamics.

Figure 8 presents the calculated data on the temperature distribution over the width ( $x$ -axis) and height ( $y$ -axis) of the cross section in the zone with internal cooling conditions. Figure 8 also shows the distribution along the length of the longitudinal section ( $z$ -axis) of the average blank and shell temperature  $T_{av}$ . The temperature of the blank was averaged over its height  $2R_1$  (Fig. 2), and in the shell — over its height  $R_1$ . According to the results of the calculation, the temperature field across the width and along the height and length of the blank has small temperature gradients and is close to a homogeneous one. Thus, the temperature drop across the blank width  $\Delta T_x \approx 100^\circ\text{C}$ ; along its height  $\Delta T_y \approx 155^\circ\text{C}$  and along the length  $\Delta T_z \approx 160^\circ\text{C}$ , which in relative units does not exceed 10%. Moreover, the good heat insulation provides almost stationary temperature conditions of synthesis products in the delay-time interval under consideration. As the delay time  $t_d$  is changed from 1 to 5 sec, the temperature of the calculation points of the longitudinal section and transverse sections decreases by no more than  $50^\circ\text{C}$ , or by about 3%. Therefore, in the first approximation, the blank within the time of a real technological cycle can be considered as a uniformly heated body with a constant temperature.

In the shell, conversely, high temperature gradients take place and localization of the high-temperature region within a narrow shell-blank contact zone is observed (Fig. 8). Let us estimate the size of the high-temperature region in which a decrease in the strain resistance of the sand shell begins to manifest itself. According to the data of [14], softening of refractive materials based on quartz forming about 95% of sand begins upon heating to a temperature above  $1000^\circ\text{C}$ . From the results of the calculations, it follows that the depth of heating the sand shell to a temperature of  $1000^\circ\text{C}$  in a time  $t_d = 5$  sec does not exceed 2 mm. Because of the insignificant size, the zone of onset of temperature softening can be neglected and it can be assumed that in the pressing process the entire volume of the sand shell maintains the initial (room) temperature.

Thus, for the real technological cycle the temperature conditions under radial SHS pressing can be considered to be quasi-stationary with a quasi-homogeneous temperature field in the blank and in the sand shell. However, the

final answer to the question on the possibility of using the approximation of the isothermal and homogeneous temperature field can be obtained by comparing the results of the calculation by the isothermal and nonisothermal models of plastic deformation.

## NOTATION

$c_i$ , specific heat capacity, J/(kg·K);  $[C]$ , heat-capacity matrix;  $dS$ , area differential;  $\{F\}$ , heat load vector;  $h_i$ , characteristic dimensions of the system's bodies, mm;  $K_1 = \sqrt{\lambda_1 c_1 \rho_1}$ ;  $K_h = \sqrt{\lambda_h c_h \rho_h}$ , criteria of thermal activity of the blank and heat insulators;  $l_1$ , length of the blank, mm;  $l_2$ , width of the shell, mm;  $n$ , normal to the boundary condition;  $R_1$ , radius of the blank, mm;  $S_4$ , area of the tool with convective heat transfer, mm<sup>2</sup>;  $T_i$ , temperature of bodies, °C;  $T_{en}$ , environment temperature, °C;  $T_c$ , combustion temperature, °C;  $T_{con.l}$  and  $T_{con.up}$ , temperature of the lower and upper contact surfaces of the blank, °C;  $T_{con0}$ , initial contact temperature, °C;  $T_{cen}$ , temperature at the blank center, °C;  $T_{eut}$ , eutectic temperature, °C;  $T_{av}$ , average temperature, °C;  $\{T_{k-1}\}$ ,  $\{T_k\}$ , matrices of the nodal temperature values at the beginning and end of the time interval  $\Delta t$ ;  $t$ , time, sec;  $t_d$ , pressing-delay time, sec;  $t_{cool}$ , cooling time, sec;  $u_c$ , rate of combustion, mm/sec;  $V_i$ , volume of the system's bodies, mm<sup>3</sup>;  $x$ ,  $y$ ,  $z$ , Cartesian coordinates;  $y_{i-1}$ ,  $z_{j-1}$ , Cartesian coordinates of the contact surface;  $z_c$ , coordinate of the burning front, mm;  $\alpha$ , heat-transfer coefficient, W/(m<sup>2</sup>·K);  $[\Lambda]$ , conduction matrix;  $\Delta t_{ck}$ , combustion time of the blank column, sec;  $\Delta z_k$ , width of the  $k$ th column of the blank, mm;  $\Delta T_x$ ,  $\Delta T_y$ ,  $\Delta T_z$ , temperature drops across the width and along the height and length of the blank, °C;  $\lambda_i$ , heat-conductivity coefficient of the system's bodies, W/(m·K);  $\rho_i$ , specific density of the system's bodies, kg/m<sup>3</sup>. Subscripts: en, environment; d, delay; con, contact; cen, center; 0, initial value; cool, cooling; con.l and con.up, lower and upper contact surfaces of the blank; av, average; h, heat insulator; eut, eutectic;  $i$ ,  $j$ , index of system's body: 1, blank, 2, sand shell, 3, tape heat insulator; 4, tool.

## REFERENCES

1. E. A. Levashov, A. S. Rogachev, V. I. Yukhvid, and I. P. Borovitskaya, *Physicochemical and Technological Principles of Self-Propagating High-Temperature Synthesis* [in Russian], Binom, Moscow (1999).
2. L. S. Stel'makh, N. N. Zhilyaeva, and A. M. Stolin, Mathematical modeling of thermal regimes of SHS force compaction, *Inzh.-Fiz. Zh.*, **63**, No. 5, 623–629 (1992).
3. A. F. Fedotov, V. P. Radchenko, and M. A. Ermolenko, Finite-element axially symmetric model of the thermal regime in the self-propagating high-temperature synthesis of blanks in a free-flowing shell, *Inzh.-Fiz. Zh.*, **75**, No. 4, 145–150 (2002).
4. L. J. Segerlind, *Applied Finite Element Analysis* [Russian translation], Mir, Moscow (1979).
5. A. V. Luikov, *Heat-Conduction Theory* [in Russian], Vysshaya Shkola, Moscow (1967).
6. G. V. Samsonov, T. I. Serebryakova, and V. A. Neronov, *Borides* [in Russian], Atomizdat, Moscow (1975).
7. A. G. Mezhanov, *Solid-Flame Combustion* [in Russian], ISMAN, Chernogolovka (2000).
8. G. N. Dul'nev and Yu. P. Zarichnyak, *Heat Conduction of Mixtures and Composite Materials* [in Russian], Energiya, Leningrad (1974).
9. A. I. Pekhovich and V. M. Zhidkikh, *Calculations of the Thermal Regime of Solid Bodies* [in Russian], Energiya, Leningrad (1976).
10. T. M. Barabarina, M. N. Sukhov, and N. A. Sheludyakov, *Glass-Fiber Building Materials* [in Russian], Izd. Literaturny po Stroitel'stvu, Moscow (1968).
11. V. P. Radchenko, A. F. Fedotov, and M. A. Ermolenko, Mechanisms of nonisothermal plastic deformation in SHS pressing, *Vestn. Samarsk. Gos. Univ.*, Issue 24, 117–124 (2004).
12. K. L. Epishin, A. N. Pityulin, and A. G. Merzhanov, Compaction of SHS-formed materials during SHS, *Poroshk. Metall.*, No. 6, 14–19 (1992).
13. V. V. Podlesov, A. V. Radugin, A. M. Stolin, and A. G. Merzhanov, Technological basis of SHS extrusion, *Inzh.-Fiz. Zh.*, **63**, No. 5, 525–537 (1992).
14. I. S. Kainarskii, *Dinas Brick* [in Russian], GNTIL po Chernoi i Tsvetnoi Metallurgii, Moscow (1961).